Dalton Transactions

Accepted Manuscript

ROYAL SOCIETY OF CHEMISTRY

www.rsc.org/dalton

$Ca_3Be_6B_5O_{16}F$: the First Alkaline-Earth Beryllium Borate with Fluorine Anions

Wenjiao Yao,[a,c] Tao Xu,[a,c] Xingxing Jiang,[a,c] Hongwei Huang,[b] Xiaoyang Wang,[a] Zheshuai Lin,*[a] Chuangtian Chen[a]

ABSTRACT: The first all-alkaline-earth beryllium borate with fluorine anions, $Ca_3Be_6B_5O_{16}F$, was synthesized by spontaneous crystallization flux method using LiF-B_2O_3 as flux. The structural framework of $Ca_3Be_6B_5O_{16}F$ is composed of the inter-connected [$Be_6B_3O_{16}$] and [BO_3] fundamental building blocks, with [CaO_7F] distorted polyhedra locating in the interstitial sites. The [$Be_6B_3O_{16}$] group is discovered for the first time in beryllium borates. The UV-Vis-NIR diffuse-reflectance spectrum demonstrates that its UV cutoff edge is below 200 nm, confirmed by the first-principles studies. Thermal analysis exposes its incongruent feature at 1321 K. IR spectroscopy measurements are consistent with the crystallographic study. These data reveal that this crystal would be applied as a deep-ultraviolet optical material.

1. Introduction

In the last decades, much attention has been focused on the exploration and characterization of inorganic borates. The main reason lies in their rich and increasing applications in laser science and technology including areas such as ultrafine spectrum analysis, precise laser micromachining and photochemical synthesis.[1-5]

Based on the structure-property relationship,[6] the multi-properties of borates originate from their rich microstructures. A boron atom can be coordinated by either three or four oxygen atoms to form a BO_3 triangle or a BO_4 tetrahedron, which can further link with each other to form a chain, layer or network by sharing corners or edges. The typical B-O microstructures include the helical chained [B_3O_7] in LiB_3O_5 (LBO),[7] quasi-layered [B_5O_9] in $NaSrB_5O_9$,[8] interconnected [BO_4] in SrB_4O_7,[9] and isolated [B_3O_6] in β-BaB_2O_4 (BBO).[10] Moreover, the incorporation of Be/Al/Si/P-O/F polyhedra can expand the structural diversity and then the application range of borates to great extent.[11-13] In particular, beryllium borates have been considered as important candidates for the ultraviolet (UV) optical materials,[14-16] as long as the *A*-site cations are alkali or/and alkaline earth cations which are free of *d*–*d* or *f*–*f* electronic transitions and exhibit very large energy bandgaps.[17-19] The incorporation of fluorine anions, due to the strong electronegativity, can further cause a blue-shift of the UV absorption edge of these crystals to the deep-UV spectral region (wavelength < 200 nm).[20] The intensive explorations in RF_n-BeO-B_2O_3 system (*R* is alkaline or/and alkaline-earth element) have given rise to the discovery of quite a few members in the alkaline or/and alkaline earth beryllium fluoroborate family which have many optoelectronic applications in the UV and deep-UV spectral region. For instance, $KBe_2BO_3F_2$ (KBBF) [21] is the sole deep-UV nonlinear optical crystal for the coherent light output at the wavelength of 177.3 nm. Nevertheless, due to weak bonding between the layers of the structure KBBF exhibits its strong layered habit in the single crystal growth processes, which heavily hinders its practical applications. The current attempts by improving the interlayer connections have resulted in the discovery of beryllium fluoroboates $NaSr_3Be_3B_3O_9F_4$[22] and *MM'*$Be_2B_2O_6F$ (*M*=Na, *M'*=Ca; *M*=K, *M'*=Ca, Sr)[23], which have been reported to have better growth habit. However, the very complicated constituents in these compounds actually make the single-crystal growth systems much more unstable. A typical example is that if the component of the melt just slightly departed from the initial ratio during the growing process, non-target compounds would be very easily obtained. Therefore, it is desirable to explore new materials in simpler systems.

Till now, the beryllium fluoroborate in which the *A*-site cations are alkaline-earth cations solely has not been discovered. The explorations in the *AE*O-BeO-B_2O_3-LiF (*AE* is alkaline earth metal) system have obtained beryllium borates such as $CaBeB_2O_5$, $Sr_3BeB_6O_{13}$, $SrBeB_2O_5$, $BaBe_2B_2O_6$, and so forth,[24-25] where the F anions are failed to enter crystal structures. In this work, through systematical investigations, the first fluorine-containing all-alkaline-earth beryllium borate, $Ca_3Be_6B_5O_{16}F$, was synthesized. The structure of $Ca_3Be_6B_5O_{16}F$ is featured by [$Be_6B_3O_{16}$] groups linking with [BO_3] groups, and [CaO_7F] distorted polyhedra are locating in the interstitial sites. The [$Be_6B_3O_{16}$] building block is first found in beryllium borates. The compound is transparent to deep-UV and easy to grow large. The synthesis, crystal structure, optical and thermal properties, and first-principles electronic band structure of $Ca_3Be_6B_5O_{16}F$ are reported.

2. Experimental and computational section

2.1 Synthesis

$CaCO_3$(AR), CaF_2(AR), BeO (99.5%), H_3BO_3 (AR), B_2O_3(99.5%), and LiF (AR) from commercial sources were used as raw materials. Because of the high toxicity

of the powder of beryllium oxide upon inhalation, all of the experiments were performed under sufficient ventilation. Single crystal was obtained by flux method through spontaneous crystallization using B_2O_3 and LiF as flux. The raw materials of $CaCO_3$, BeO, B_2O_3, and LiF in the original ratio of 2:1:2:2 were carefully ground and mixed in an agate mortar and packed into a platinum crucible and gradually heated to 1273 K in a self-made furnace. Additional B_2O_3 and LiF were added to adjust the viscosity and the volatility of the melt. The melt were then kept at that temperature with interval stir for at least 24 h to ensure homogeneous. The temperature was then lowered at a rate of 10 K per day until the mixture was curdled. The crucible was then taken out of the furnace and cooled to room temperature in air. Many colorless, transparent block crystals were obtained for later tests. We found that the content of BeO and LiF is crucial to synthesize the title compound; if the content of Be is low the crystals free of Be, e.g., CaB_2O_4, $Ca_5B_3O_9F$, would be obtained, while if the content of LiF is low, the crystals free of F, e.g., $CaBeB_2O_5$, would be obtained. The traditional method of high temperature solid state reaction was also carried out with the stoichiometric ratio of $CaCO_3$, CaF_2, BeO, and H_3BO_3, topped to 1400 K. The temperature precision was stabilized within 0.1 K.

2.2 **Structural Determination**

Single crystal X-ray diffraction data for $Ca_3Be_6B_5O_{16}F$ was generated from graphite-monochromatized Mo-Kα radiation (λ=0.71073 Å) at 153 K on a Rigaku AFC10 single-crystal diffractometer and collected with Saturn CCD detector. A colorless, transparent crystal with dimensions of 0.32 × 0.31 × 0.20 mm^3 was selected for structure determination. Crystalclear program was run to record the intensity data and perform cell refinement and data reduction. The structure was solved with Shelxtl-97[26] by the direct method and refined by full-matrix least-squares techniques with anisotropic thermal parameters. A summary of crystal data and structure refinement for the title compound is listed in Table 1. The atomic coordinates and uniformized thermal factor are summarized in Table 2.

2.3 **Element analysis**

The inductively coupled plasma optical emission spectrometer (ICP-OES) analysis was carried out to semi-quantitatively determine its composition. The crystal samples were dissolved in dilute hydrochloric acid (5 mL) with water-bath heating. The test was performed on a Varian 710-ES with Sepex Certiprep standards, which reveals Ca:Be:B = 1:1.903:1.627.

2.4 **X-ray powder diffraction**

The powder X-ray diffraction (PXRD) pattern was recorded with a Bruker D8 advanced X-ray diffractometer using Cu K*α* radiation (λ = 1.5418 Å). The as-grown crystals were ground to fine polycrystal in an agate mortar. The powder diffraction pattern was recorded in the angular range from 5° to 75° with a scanning step width of 0.02° and at rate of 0.2°/s. Theoretical simulation were also carried out based on single crystal crystallographic data.

2.5 **Thermal analysis (Differential scanning calorimetry, DSC)**

The thermal property of the title compound was investigated by differential scanning calorimetric (DSC) measurements. Ground crystals of the title compound were used as subject. In detail, a sample (about 10 mg) of ground crystal was placed in a platinum crucible and heated in a Labsys TG-DTA16 (SETARAM) thermal analyzer from room temperature to 1523 K at a rate of 10 K /min in nitrogen atmosphere. Al_2O_3 powder as commercial received was applied as calibration.

2.6 **IR Spectroscopy**

IR spectroscopy was carried out with the objective of specifying and comparing the coordination of boron in the title compound. The mid-infrared spectrum was obtained at room temperature via a Bio-Rad FTS-60 FTIR spectrometer. The sample and dried KBr at the weight ratio of about 1:100 were mixed thoroughly together. The spectrum was collected in a range from 400 to 4000 cm^{-1} with the resolution of 1 cm^{-1}.

2.7 **UV-Vis-NIR Diffuse-Reflectance Spectroscopy**

UV-Vis-NIR diffuse-reflectance data for the title compound were collected with a SolidSpec-3700 DUV spectrophotometer in the wavelength range from 200 to 2600 nm. Fluororesin is applied as the standard.

2.8 **First principles calculations**

The first-principles electronic structure calculations were performed by CASTEP,[27] a total energy package based on density functional theory (DFT)[28] with plane wave pseudopotential method. The functionals in generalized gradient approximation (GGA)[29] developed by Perdew, Burke and Ernzerhof (PBE)[30] were adopted to describe the exchange-correlation (XC) energy. The optimized norm-conserving pseudopotential[31] in Kleinman-Bylander[32] form allow us to use a relatively small basis without compromising the computational precision, in which Ca $3s^23p^64s^2$, Be $2s^2$, B $2s^22p^1$, O $2s^22p^4$ and F $2s^22p^5$ electrons are treated as valence electrons. The high kinetic energy cutoff 900 eV and dense Monkhorst-Pack[33] *k*-point meshes spanning less than 0.04 $Å^{-1}$ in the Brillouin zone were chosen. Our convergence test showed that the choice of computational parameters is sufficiently accurate in this study.

3. Results and discussion

3.1 **Crystal Structure**

The $Ca_3Be_6B_5O_{16}F$ crystallizes in the hexagonal system with the centrosymmetric space group of P*63m* (No. 176). The framework viewed along the *c*-axis is illustrated in Figure 1a. In the symmetric unit, Ca, Be, B, O, F each occupies one, one, two, four and one crystallographically unique position, respectively. All B(1) or Be atoms are coordinated to four O atoms to form the tetrahedral groups. Three $B(1)O_4$ tetrahedra and six BeO_4 tetrahedra are alternately connected together by sharing edges or corners, constructing a novel hexagonal prism-like $[Be_6B_3O_{16}]$ group. Meanwhile, a B(2) atom is coordinated to three O atoms to form a planar BO_3 unit in the *a-b* plane, and a Ca atom is coordinated with seven O atoms and one F atom to form a $[CaO_7F]$ polyhedron. Overall, the structure is characterized by a complicated three-dimensional (3D) network composed of the

$[Be_6B_3O_{16}]$ groups linked with $[BO_3]$ triangles, while the distorted $[CaO_7F]$ polyhedra are located in the interstices. In order to define unambiguously the coordination polyhedra, the bond valence sums (BVS) for all ions were calculated and listed in Table 2, which show good agreement with the formal atom charges.

The $[Be_6B_3O_{16}]$ group is found for the first time in beryllium borates, where the B(1)-O bond lengths vary from 1.474 Å to 1.489 Å and O-B-O bond angles from 104.73° to 113.67 °, while the Be-O bond lengths range from 1.618 Å to 1.704 Å and O-Be-O bond angles from 104.38° to 114.13°. It is interesting that along the *c* axis three of the constituent BeO_4 tetrahedra are right over another three BeO_4 (Figure 1b), and the adjacent $[Be_6B_3O_{16}]$ groups are rotated by 60° in the *ab* plane and linked together by sharing O(2) atoms (Figure 1c). Each of six O(3) atoms of a $[Be_6B_3O_{16}]$ group is bridged to a $[BO_3]$ group and therefore form the three-dimensional framework. For the $[BO_3]$ triangles which interconnect the $[Be_6B_3O_{16}]$ groups the B-O bond lengths and O-B-O bond angles are uniformly 1.382 Å and 119.98°, respectively. The average bond lengths and bond angles in the $[Be_6B_3O_{16}]$ and $[BO_3]$ groups are comparable to those in other beryllium borates. [21-25, 34-38]

In the distorted $[CaO_7F]$ polyhedron, a Ca^{2+} cation is coordinated to four O(2) atoms, two O(3) atoms, one O(4) atom and one F atom, as depicted in Figure 2a. The Ca-O bond lengths range from 2.357 Å to 2.668 Å, and O-Ca-O angles from 63.05° to 148.44°, while the Ca-F bond length is 2.218 Å. The connection of the $[CaO_7F]$ polyhedron to other groups is quite complex. For each $[CaO_7F]$ polyhedron, it is corner-jointed to three $(Be/B)O_4$ tetrahedra by one O(4) atom, and other five $(Be/B)O_4$ tetrahedra by two O(3) atoms. As viewed along the *c*-axis, twelve $[CaO_7F]$ polyhedra construct a large ring, which perfectly encircles two $[Be_6B_3O_{16}]$ groups (shown in Figure 2b). Each $[CaO_7F]$ polyhedron connects with the two neighboring $[CaO_7F]$ groups along the *c*-axis by sharing common edges, while links to another two $[CaO_7F]$ groups in *ab* plane via a F atom, as shown in Figure 2c.

It is interesting that the structure of the title compound is quite different from the other members in the alkaline or/and alkaline earth beryllium fluoroborate family, especially with respect to the coordination environments of boron and fluorine atoms. Figure 3 displays the comparison of the crystal structures between $Ca_3Be_6B_5O_{16}F$ and the other members in the alkaline or/and alkaline earth beryllium fluoroborate family, such as KBBF, $NaCaBe_2B_2O_6F$, and $NaSr_3Be_3B_3O_9F_4$. It is clearly shown that (i) in the compounds containing the alkaline cations, all B atoms are congruously coordinated to three O atoms to form planar triangles. These groups are further bridged by BeO_4/BeO_3F polyhedra, forming the layer-like frameworks. As a comparison, in the title compound, although two out of five B atoms are three-coordinated and coplanar arranged, the rest are four-coordinated and the layer tendency is broken. (ii) In the latter three compounds, F atoms participate in the construction of BeO_3F tetrahedra by linking with the Be atom(s), although the coordination number around a F atom varies from one, two to three, as in KBBF, $NaCaBe_2B_2O_6F$, $NaSr_3Be_3B_3O_9F_4$, respectively. In $Ca_3Be_6B_5O_{16}F$, however, all F atoms are merely connected with Ca atoms rather than with Be atoms.

3.2 Thermal analysis and PXRD analysis

The thermal analysis on crystalline $Ca_3Be_6B_5O_{16}F$ exhibits a strong endothermal peak at 1321 K, as indicated by DSC curve in Figure 4a. The PXRD pattern of the title compound is drawn in Figure 4b. From the picture, we see that the pattern of crystalline $Ca_3Be_6B_5O_{16}F$ shows good agreement with the calculated one derived from the single crystal data. The crystalline powder was then heated above 1321 K (around 1373 K) and PXRD pattern was taken again on the residuary. The pattern shows a mixture of glass phases and CaB_2O_4, which reveals the incongruent melting compound behavior of the title compound. The PXRD of the synthetic powders from solid-state reaction shows mainly the peaks of CaF_2, indicating that the compound cannot be obtained by high temperature solid-state reaction.

3.3 IR and UV-Vis-NIR Diffuse-Reflectance Spectroscopy

The IR Spectroscopy spectrum of crystalline $Ca_3Be_6B_5O_{16}F$ is shown in Figure 5a. The main infrared absorption band at 1311 cm^{-1} is assigned to the asymmetric stretching vibration of the triangular borate groups, whereas the band at 1109 cm^{-1} is the in-plane bending of B-O in BO_3. The bands around 1000 cm^{-1} (1028 and 966) originate from the asymmetric and symmetric stretching vibration of BO_4 group. Those in the range of 885–692 cm^{-1} might attribute to the banding modes of BO_3 group. Peaks at 482 cm^{-1}, 536 cm^{-1}, and 632 cm^{-1} are the bending modes of BO_3 group. The present measurements are consistent with the results for other borates.[39-45] It validates the existence of the different borate groups in the crystal structure.

Figure 5b displays the UV-Vis-NIR Diffuse-Reflectance Spectrum of $Ca_3Be_6B_5O_{16}F$, which illustrates high transparency in the UV region and cut-off wavelength extending to lower than 200 nm, suggesting the potential of this crystal for the UV and deep-UV applications.

3.4 Electronic structure calculations

Figure 6 shows the GGA calculated electronic structure in the title compound. The electronic band structure reveals that $Ca_3Be_6B_5O_{16}F$ is an indirect band gap insulator with an underestimated band gap of 4.9 eV due to the discontinuity of the GGA functionals. In order to overcome this problem, the energy bandgap calculations by the DFT with hybrid XC functionals (e.g., PBE0[43]) and by the recently developed MBVS method,[44] both of which have the capability to accurately predict the energy band gaps in UV borates,[44-46] have been performed. The calculated results reveal that the energy band gap of $Ca_3Be_6B_5O_{16}F$ is about 7 eV (or UV cutoff wavelength of 175 nm), confirming the experimental measurement.

According to the partial density of states (PDOS), several electronic characteristics can be obtained: (1) the Ca 2s electrons are localized strongly at 38.0eV, which is difficult to stimulate by external perturbation. (2) the energy band between -30.0 and -15.0 eV is mainly composed of Ca 4p, Be 2p, B 2s 2p ,O 2s and F 2s. The sharp peak of Ca 4p occurs at -20.0 eV, overlapping little with other orbitals, which indicates the strong iconicity of calcium. (3) the Be 2p ,B 2p and O 2p contribute mostly

to the top of valence band(VB),i.e., -10eV~0eV. The wide energy range of hybridization among these orbitals shows the strongly covalent properties of B-O bonds and Be-O bonds. The conduction band (CB) bottom is composed of Be 2p, B 2p and O 2p, while the orbital of calcium also have considerable contribution. It is clear that the energy bandgap of $Ca_3Be_6B_5O_{16}F$ is mainly determined by the $[Be_6B_3O_{16}]$ group which thus would have dominant contribution to the optical properties of crystal in the UV and deep-UV region.

4. Conclusion

The first alkaline-earth beryllium fluoroborate was discovered in the CaO-CaF_2-BeO-B_2O_3 system. This compound crystallizes in the hexagonal system, centrosymmetric P*63m* space group. The framework of $Ca_3Be_6B_5O_{16}F$ is constructed by a three-dimensional network with interconnected $[BO_3]$ groups, $[Be_6B_5O_{16}]$ groups, and $[CaO_7F]$ polyhedra. The $[Be_6B_5O_{16}]$ group in the structure is found for the first time in the beryllium borates. The crystal melts incongruently and the UV cut-off edge is lower than 200 nm. This work may benefit the succeeding exploration in alkaline earth fluorine beryllium borates. Further investigation for growing large crystals and related novel compounds are in process.

Acknowledgement

The authors acknowledge the useful discussions with Gong, Pifu; Xia, Mingjun; Liu, Lijuan. This work was supported by the National Natural Science Foundation of China under Grant Nos 11174297, 91022036, and 51302251, the Fundamental Research Funds for the Central Universities (2652013052), and the National Basic Research Project of China (Nos 2010CB630701 and 2011CB92204).

Notes and references

[a] Technical Institute of Physics and Chemistry, Chinese Academy of Sciences, Beijing 100190, China. Fax: 86-10-82543709; Tel: 86-10-82543718; E-mail: zslin@mail.ipc.ac.cn
[b] School of Materials Science and Technology, China University of Geosciences, Beijing 10083, PR China.
[c] University of Chinese Academy of Sciences, Beijing 100049, China.

Electronic Supplementary Information (ESI) available: Crystallographic data of $Ca_3Be_6B_5O_{16}F$. See DOI: 10.1039/b000000x/

1. Petra Becker, *Adv. Mater.*, 1998, **10**, 979-992.
2. T. Kiss, F. Kanetaka, T. Yokoya, T. Shimojima, K. Kanai, S. Shin, Y. Onuki, T. Togashi, C. Zhang, C.T. Chen, S. Watanabe, *Phys. Rev. Lett.*, 2005, **94**, 057001.
3. R. D. Schaeffer, T. Hannon, *Laser Focus World,* 2001, **37**, 115; D. Cyranoski, *Nat.,* 2009, **457**, 953.
4. Atsuo Yamada, Nobuyuki Iwane, Yu Harada, Shin-ichi Nishimura, Yukinori Koyama, and Isao Tanaka, *Adv. Mater.*, 2010, **22**, 3583-3587.
5. T. Sekikawa, A. Kosuge, T. Kanai, S. Watanabe, *Nat.,* 2004, **432**, 605.
6. C. T. Chen, Y. B. Wang, Y. N. Xia, B. C. Wu, D. Y. Tang, K. C. Wu, W. R. Zeng, L. H. Yu, L. F. Mei, *J. Appl. Phys.,* 1995, **77** (6), 2268-2272.
7. C. T. Chen, Y. C. Wu, A. D. Jiang, B. C. Wu, G. M. You, R. K. Li and S. J. Lin, *J. Opt. Soc. Am. B-Opt. Phys.*, 1989, **6**, 616-621.
8. L. Wu, Y. Zhang, X.L. Chen, Y.F. Kong, T.Q. Sun, J.J. Xu, Y.P. Xu, *J. Sol. Sta. Chem.*, 2007, **180**, 1470–1475.
9. Yu. S. Oseledchik, A. L. Prosvimin, A. I. Pisarevskiy, V. V. Starshenko, V. V. Osadchuk, S. P. Belokrys, N. V. Svitanko, A. S. Korol, S. A. Krikunov, A. F. Selevich, *Opt. Mater.*, 1995, **4**, 669-674.
10. C. T. Chen, B. C. Wu, A. D. Jiang, G. M. You, *Sci. Sinica B,* 1985, **28**, 235-243.
11. H. P. Wu, H. W. Yu, Z. H. Yang, X. L. Hou, X. Su, S. L. Pan, K. R. Poeppelmeier, J. M. Rondinelli, J. *Am. Chem. Soc.,* 2013, **135**, 4215-4218.
12. H. P. Wu, H. W. Yu, Z. H. Yang, S. L. Pan, Z. J. Huang, X. Su, K. R. Poeppelmeier, *Angew. Chem. Int. Ed.*, 2013, **52**, 3406-3410.
13. W. Yu , H. P. Wu , S. L. Pan , Z. H. Yang, X. Su, F. F. Zhang, *J. Mater. Chem.,* 2012, **22**, 9665-9670.
14. R. T. Mu, Q. Fu, L. Jin, L. Yu, G. Z. Fang, D. L. Tan, and X. H. Bao, *Angew. Chem. Int. Ed.,* 2012, **51**, 4856 –4859.
15. Y. M. Xu, P. Richard, K. Nakayama, T. Kawahara, Y. Sekiba, T. Qian, M. Neupane, S. Souma, T. Sato, T. Takahashi, H.-Q. Luo, H.-H. Wen, G.-F. Chen, N.-L. Wang, Z. Wang, Z. Fang, X. Dai& H. Ding, *Nat. Comm.,* 2011, **2**, 392.
16. Y. M. Xu, Y. B. Huang, X. Y. Cui, E. Razzoli, M. Radovic, M. Shi, G. F. Chen, P. Zheng, N. L. Wang, C. L. Zhang, P. C. Dai, J. P. Hu, Z. Wang, H. Ding, *Nat. Phys.*, 2011, **7**, 198-202.
17. C. T. Chen, *Sci. Sin.* 1979, **22**, 756-766.
18. R. K. Li, *J. Non-Cryst. Solids,* 1989, **111**, 199-204.
19. C. T. Chen, Y. C. Wu, R. K. Li, *Int. Rev. Phys. Chem.* 1989, **8**, 65.
20. M. Luo, N. Ye, G. H. Zou, C. S. Lin, W. D. Cheng, *Chem. Mater.* 2013, **25**, 3147-3153.
21. C. T. Chen, G. L. Wang, X. Y. Wang, Z. Y. Xu, *Appl. Phys. B,* 2009, **97**, 9.
22. H. W. Huang, J. Y. Yao, Z. H. Lin, X. Y. Wang, R. He, W. J. Yao, N. X. Zhai, C. T. Chen, *Angew. Chem. Int. Ed.*, 2011, **50**, 9141-9144.
23. H. W. Huang, J. Y. Yao, Z. H. Lin, X. Y. Wang, R. He, W. J. Yao, N. X. Zhai, C. T. Chen, *Chem. Mater.*, 2011, **23**, 5457-5463.
24. K. I. Schaffers, D. A. Keszler, *Acta Crystallogr. C*, 1993, **49**, 647–650; K. I. Schaffers, D. A. Keszler, *Inorg. Chem.*, 1994, **33**, 1201-1204.
25. W. J. Yao, H. W. Huang, J. Y. Yao, T. Xu, X. X. Jiang, Z. S. Lin, C. T. Chen, *Inorg. Chem.,* 2013, **52**, 6136−6141; W. J. Yao, X. S. Wang, H. W. Huang, T. Xu, X. X. Jiang, X. Y. Wang, Z. S. Lin, C. T. Chen, *J. Alloys Compd.,* 2013, **593**, 256-260.
26. G. M. Sheldrick, *SHELXS–97, Program for X-ray Crystal Structure Solution*, University of Gottingen: Gottingen, Germany, 1997.
27. S. J. Clark, M. D. Segall, C. J. Pickard, P. J. Hasnip, M. J. Probert, K. Refson, M. C. Payne, *Z. Kristallogr.* 2005, **220** (5-6), 567-570.
28. W. Kohn, L. J. Sham, *Rev. Mod. Phys.*, 1999, **71**, 1253-1266.
29. J. P. Perdew, Y. Wang, *Phys. Rev. B,* 1992, **45**, 13244-13249.
30. J. P. Perdew, K. Burke, *Phys. Rev. Lett.,* 1996, **77**, 3865-3868.
31. A. M. Rappe, K. M. Rabe, E. Kaxiras, J. D. Joannopoulos, *Phys. Rev. B,* 1990, **41** (2), 1227-1230.
32. L. Kleinman, D. M. Bylander, *Phys. Rev. Lett.,* 1982, **48** (20), 1425-1428.
33. H. J. Monkhorst, J. D. Pack, *Phys Rev B,* 1976, **13** (12), 5188-5192.
34. S. C. Wang, N. Ye, W. Li, D. Zhao, *J. Am. Chem. Soc.,* 2010, **132**, 8779.
35. H. W.Huang, L. J. Liu, S. F. Jin, W. J. Yao, Y. H. Zhang, C. T. Chen, *J. Am. Chem. Soc.,* 2013, **135**, 18319-18322.
36. S. C. Wang, N. Ye, *J. Am. Chem. Soc.,* 2011, **133**, 11458-11461.
37. C. T. Chen, S. Y. Luo, X. Y. Wang, G. L. Wang, X. H. Wen, H. X. Wu, X. Zhang,; Z. Y. Xu, *J. Opt. Soc. Am. B-Opt. Phys.,* 2009, **26**, 1519-1525.
38. H. W. Huang, C. T. Chen, X. Y. Wang, Y. Zhu, G. L. Wang, X. Zhang, L. R. Wang, J. Y. Yao, *J. Opt. Soc. Am. B-Opt. Phys.,* 2011, **28**, 2186-2190.
39. R. Cong, J. L. Sun, T. Yang, M. R. Li, F. H. Liao, Y. X. Wang and J. H. Lin, *Inorg. Chem.,* 2011, **50**, 5098-5104.
40. X. Y. Fan, S. L. Pan, X. L. Hou, X. L. Tian, J. Han, J. Haag and K. R. Poeppelmeier, *Cryst. Growth Des.,* 2010, **10**, 252-256.
41. Y. Yang, S. L. Pan, J. Han, X. L. Hou, Z. X. Zhou, W. W. Zhao, Z. H. Chen, M. Zhang, *Cryst. Growth Des.,* 2011, **11**, 3912-3916.

42. Y. Yang, S. L. Pan, X. L. Hou, X. Y. Dong, X. Su, Z. H. Yang, M. Zhang, W. W. Zhao and Z. H. Chen, *Cryst. Eng. Comm.*, 2012, **14**, 6720-6725.
43. C. Adamo, V. Barony, *Chem. Phys. Lett.,* 1998, **298**, 113-119.
44. R. He, H. W. Huang, L. Kang, W. J. Yao, X. X. Jiang, Z. S. Lin, J. G. Qin, C. T. Chen, *Appl. Phys. Lett.,* 2013, **102**, 23, 1904.
45. Z. S. Lin, L. Kang, T. Zheng, Ran He, H. Huang, C. T. Chen, *Comput. Mater. Sci.,* 2012, **60**, 99-104.
46. R. He, Z. S. Lin, T. Zheng, H. Huang, C. T. Chen, *J. Phys. Condens. Matt.*, 2012, **24**, 14, 5503.

Table 1 Crystallographic data for $Ca_3Be_6B_5O_{16}F$.

Formula	$Ca_3Be_6B_5O_{16}F$
Formula weight	503.35 g/mol
Crystal system	hexagonal
Space group	*P*63m (*No.*176)
Unit cell parameters	*a*= 8.9753(13) Å,
	c =7.7356(15) Å,
	V=539.66(15) Å^3,
	Z=2
Index ranges	$-11 \le h \le 13$,
	$-13 \le k \le 11$,
	$-9 \le l \le 11$
d_{calc} (g/cm^3)	3.10
θ range	2.6205-31.4816°
No. of reflections	5363
No. of refined parameters	2344
R indices (all data)	0.0264/0.0644
Final R indices *[I > 2σ(I)]*	0.0259/0.0641
Goodness-of-fit on F^2	1.294

Table 2 The atomic coordinates and calculated bond valence sum (BVS).

Atom	Wyck.	Site	x/a	y/b	z/c	U [Å^2]	BVS
Ca1		m.	0.46368(5)	1.51200(5)	1/4	0.0050(52)	1.937
O1	2a	-6.	0	1.00000	1/4	0.0034	1.962
O2	12i	1	0.51710(12)	1.34172(13)	0.05572(14)	0.0064(07)	2.099
O3	12i	1	0.20287(12)	1.26703(12)	0.09915(13)	0.0050(07)	2.0023
O4	6h	m.	0.76652(17)	1.71059(18)	1/4	0.0054(27)	1.880
F1	2c	-6.	1/3	1.66670	1/4	0.0098(07)	1.086
B1	6h	m.	0.0882(3)	1.1963(3)	1/4	0.0039(5)	2.897
B2	4f	3.	2/3	1.33330	0.0531(4)	0.0062(1)	2.914
Be1	12i	1	0.1441(2)	1.3238(2)	-0.0710(2)	0.0047(7)	2.005

Fig. 1 Crystal structure of $Ca_3Be_6B_5O_{16}F$. (a) Sketched network, where the black box is a unit cell; (b) The $[Be_6B_3O_{16}]$ group; (c) Connection between $[Be_6B_3O_{16}]$ groups, where for the sake of clarification the corner shared O atoms (O2) between two $[Be_6B_3O_{16}]$ groups are split, and connected by the dashed lines. Gold and blue polyhedra represent $[BO_4]$ and $[BeO_4]$ groups, respectively. The light and dark shades indicate the groups in high and low layers, respectively, viewed along the *c*-axis.

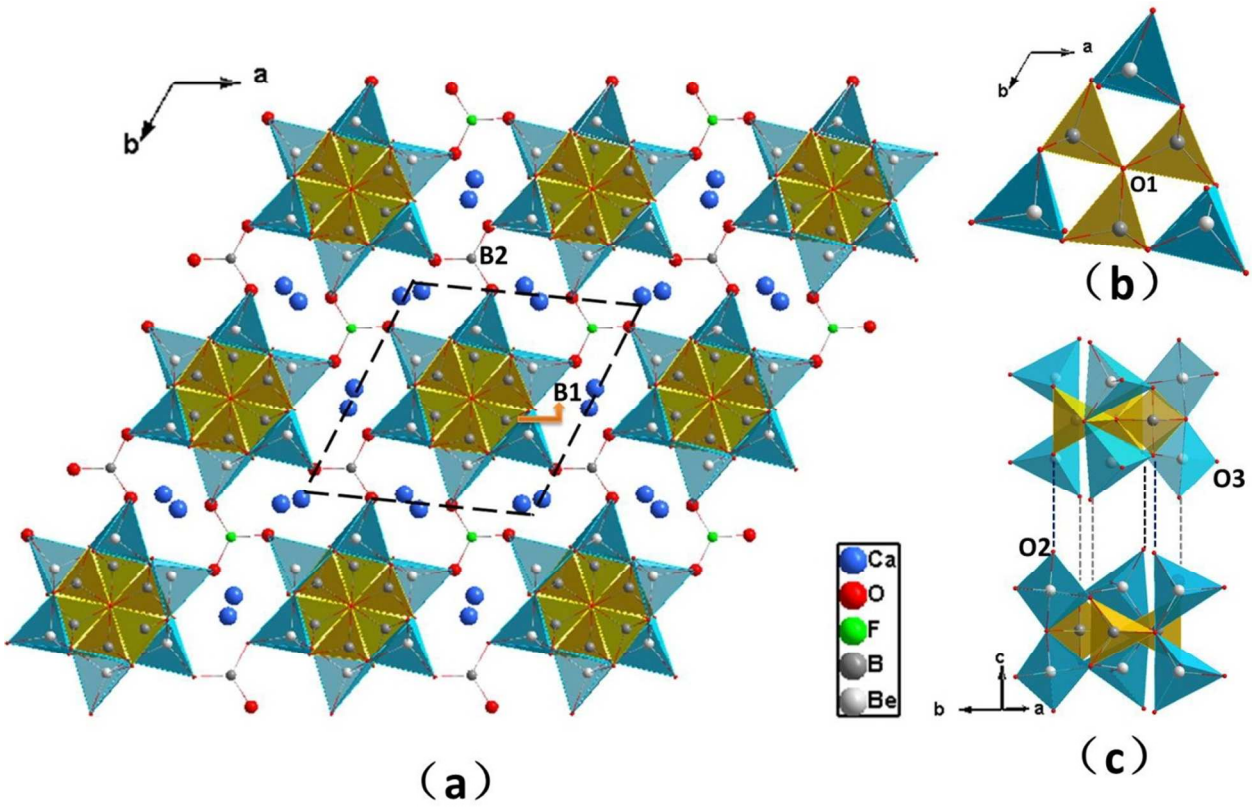

Fig. 2 Coordination environments of: (a) $[CaO_7F]$ polyhedron and basic anionic groups; (b) $[CaO_7F]$ polyhedra to $[Be_6B_3O_{16}]$ groups; (c) $[CaO_7F]$ polyhedron to other $[CaO_7F]$ polyhedral in the *a*-*c* plane (left) and in the *a*-*b* plane (right). Gold, blue, and pink polyhedra represent $[BO_4]$, $[BeO_4]$, and $[CaO_7F]$ groups, respectively. The light and dark shades indicate the groups in high and low layer, respectively, viewed along the *c*-axis.

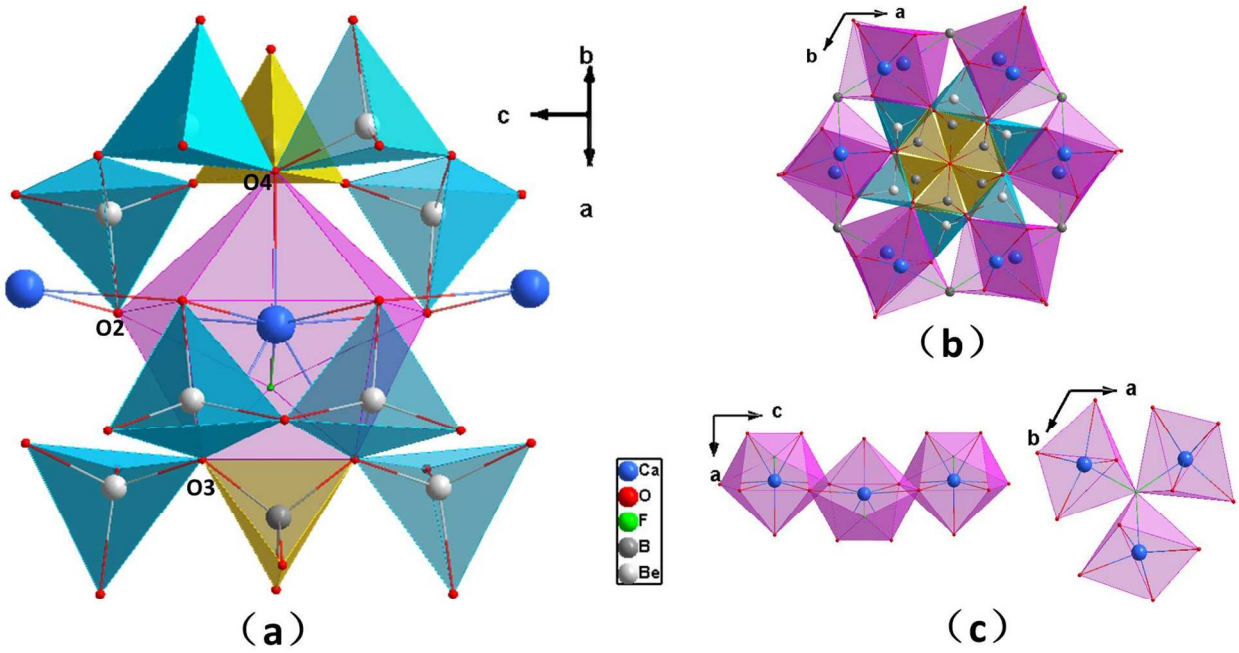

Fig. 3 Different coordination environments for B and F atoms in (a) KBBF; (b) $NaCaBe_2B_2O_6F$; (c) $NaSr_3Be_3B_3O_9F_4$; (d) $Ca_3Be_6B_5O_{16}F$. Pink, gold, green, and blue polyhedra represent $[CaO_7F]$, $[BeO_3F]$, $[BO_4]$, and $[BO_3]$ groups, respectively.

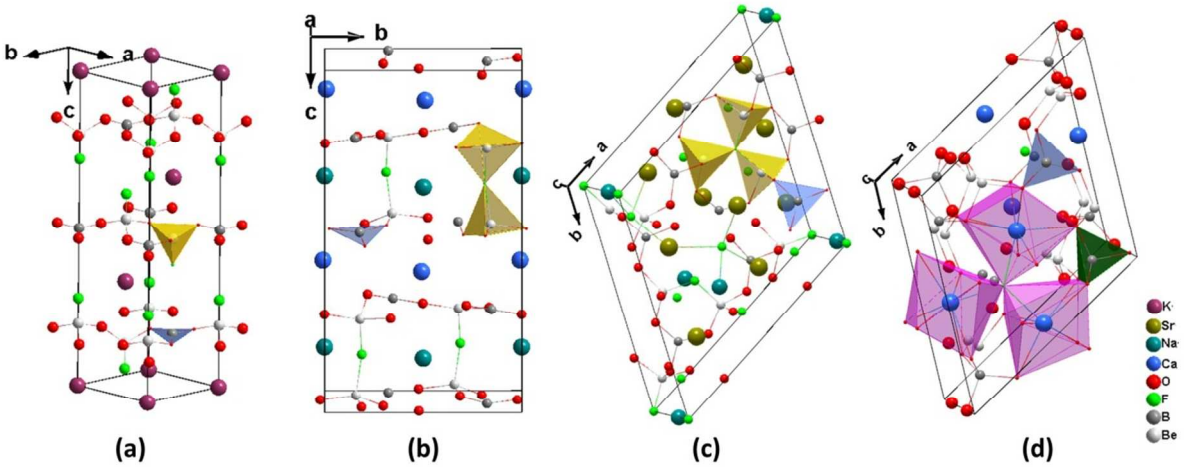

Fig. 4 Physical characterization of $Ca_3Be_6B_5O_{16}F$. (a) DSC curve (b) Powder XRD patterns.

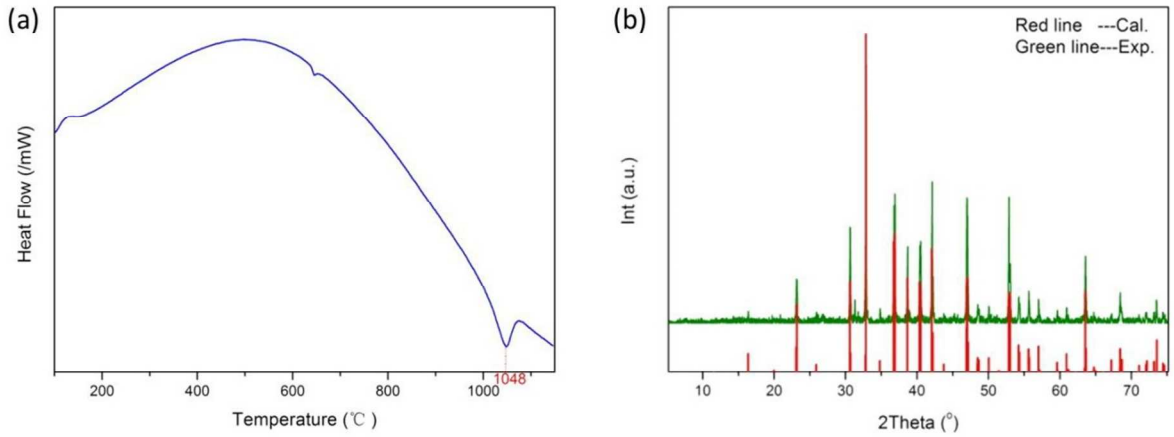

Fig. 5 Physical characterization of $Ca_3Be_6B_5O_{16}F$ (a) IR spectrum (b) UV-Vis-NIR Diffuse-Reflectance Spectrum.

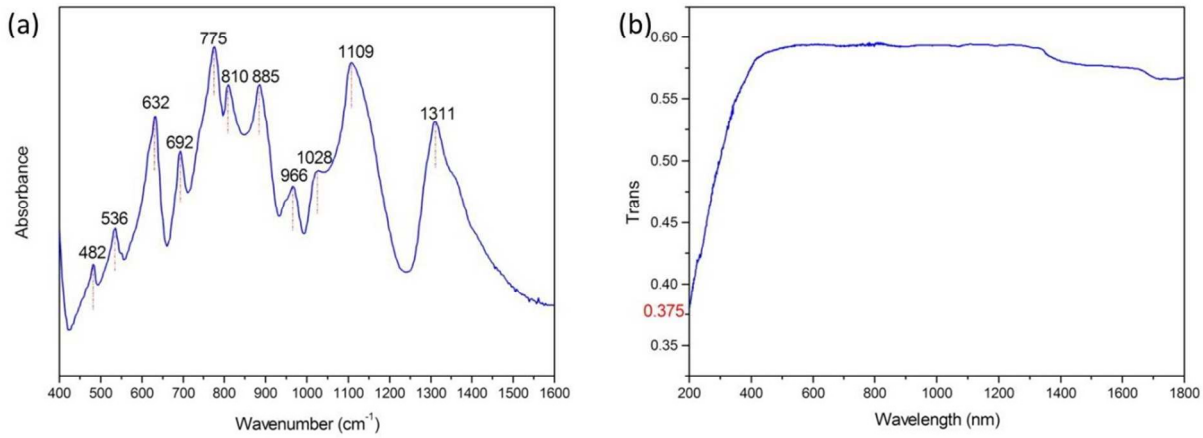

Fig. 6 Electronic band structure (left) and Partial density of states (PDOS) (right) of $Ca_3Be_6B_5O_{16}F$.

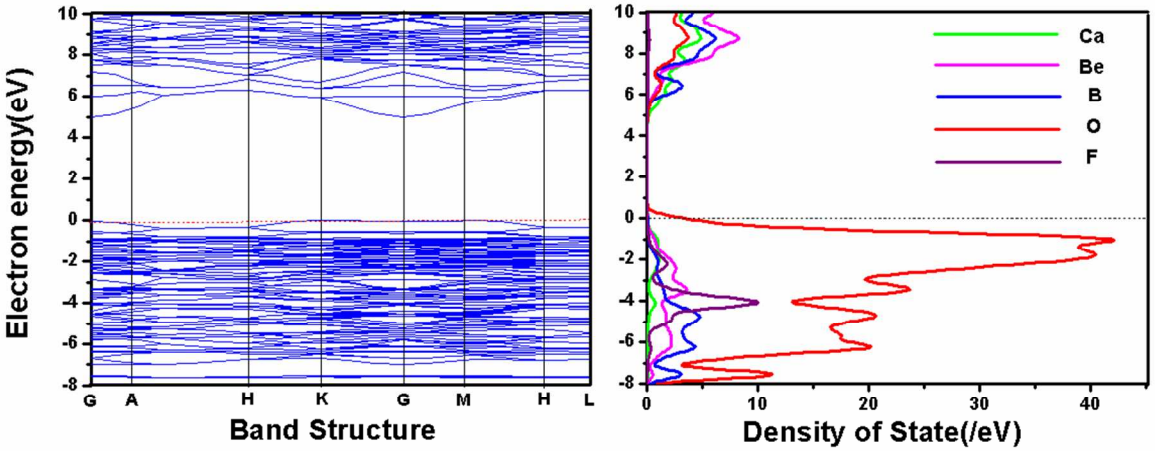

TOC